

Mechanistic Insights on the Neuro-Modulatory Potential of *Cannabis sativa*: A Network Pharmacology- and Molecular Dynamics Simulation-Based Approach

Christina Peter¹, Halimat Yusuf Lukman¹, Nosipho Wendy S'thebe¹, Usman Abiola Sanni^{2,3}, Saheed Sabiu^{1*}

Christina Peter¹, Halimat Yusuf Lukman¹, Nosipho Wendy S'thebe¹, Usman Abiola Sanni^{2,3}, Saheed Sabiu^{1*}

¹Department of Biotechnology and Food Science, Faculty of Applied Sciences, Durban University of Technology, P. O. Box 1334, Durban 4000, SOUTH AFRICA

²Department of Paediatrics, Federal Medical Centre, Birnin Kebbi, Nigeria, WEST AFRICA

³Partners in Health, Koidu, Kono, Sierra Leone, WEST AFRICA

Correspondence

S. Sabiu

Department of Biotechnology and Food Science, Faculty of Applied Sciences, Durban University of Technology, P. O. Box 1334, Durban 4000, SOUTH AFRICA

Email: Sabius@dut.ac.za

History

- Submission Date: 10-07-2025;
- Review completed: 13-08-2025;
- Accepted Date: 25-08-2025.

DOI : 10.5530/pj.2025.17.51

Article Available online

<http://www.phcogj.com/v17/i4>

Copyright

© 2025 Phcogj.Com. This is an open-access article distributed under the terms of the Creative Commons Attribution 4.0 International license.

ABSTRACT

Background: Although, studies have reported the use of cannabis as a temporary antidepressant and implicated its chronic use in neurological diseases, the exact mechanisms through which these happen remain elusive. **Objective:** This study aims to investigate the neuro-modulatory potential of cannabis as antidepressant and its role in neurological disorders. **Methodology:** Network pharmacology and molecular dynamics simulation were employed to unveil the mechanism of cannabis as a temporary antidepressant and potential agent implicated in neurological disorders. **Results:** A total of 156 cannabis metabolites were retrieved from data mining. 22 genes were common in cannabis metabolites and central nervous system (CNS) neurotransmitters' genes. Glutamate receptor activity and neuroactive ligand receptor activity (NALR) were the most enriched biological process and signalling pathway, respectively, with cannabinoid receptor 1 (*CNR1*) and glutamate metabotropic receptor 2 (*GRM2*) being the hub targets in the NALR pathway. A probe into the structural stability of top-ranked metabolites identified cholesterol-*CNR1* (-73.88 kcal/mol) and campesterol-*CNR1* (-65.96 kcal/mol) with lower free binding energy than reference antidepressant drug (anandamide) (-65.08 kcal/mol), whereas for *GRM2*, the binding free energy of nerolidol (-43.57 kcal/mol) which was the least among the top ranked metabolites was higher compared to anandamide (-58.78 kcal/mol). **Conclusion:** Data from this study shows that the profiled cannabis metabolites displayed modulatory effects on key neurotransmitters of the CNS and their receptors and formed stable binding interaction with genes implicated in brain functioning suggestive of the mechanistic effect of cannabis on brain activity during depression and chronic use.

Keywords: Cannabis, Cannabinoid receptors, Depression, Neurological diseases, Neurotransmitters

INTRODUCTION

Within the realm of therapeutics, drugs derived from herbal remedies with effects on cognitive and behavioural processes fall under the branch of psychopharmacology¹. The interest in psychopharmacology has led to the development of antidepressants, anxiolytics, antipsychotics, mood stabilisers, and euphoria inducing stimulants for therapeutic purposes². These drugs penetrate the blood brain barrier and act by modifying neuronal functions³. Plants containing psychoactive substances are often used as antidepressants⁴ with *Hypericum perforatum*, *Agapanthus campanulatus* and *Cannabis sativa* heralded among the most studied plants with antidepressant properties⁵. Due to its psychedelic effects, *Cannabis sativa* is often classified as a euphoric stimulant against depression and depressive-like symptoms with an estimated 4.3% (219 million) global users^{6,7}. The use of cannabis is not limited to Africa and developing countries only, in some developed countries such as the United State of America, its use has been legalized for recreational purposes in 17 states and for medicinal purposes in 36 states since April 2021⁸.

Cannabis sativa L. (cannabis) is an ancient plant used traditionally to treat menstruation, absentmindedness, tetanus, rabies, rheumatism, and convulsions⁸. Other reported uses include the treatment of glaucoma, epilepsy, insomnia,

inflammation, multiple sclerosis, nausea, seizures, and asthma⁹. Over 100 phytoconstituents including terpenes, phenolics, Δ^9 -tetrahydrocannabinol (THC) and cannabidiol (CBD), have been identified in cannabis. However, THC causes the "high" feeling experienced by users while CBD is non-psychoactive⁸. Like other psychoactive drugs, cannabis metabolites have the inherent ability to modulate the neurotransmitters (NTs) by mimicking the natural NTs. The drugs can bind and activate nerve cells in a way different from the natural NTs resulting in the transmission of abnormal signals, prevention of normal cycle/recycling of the natural NTs, and enhance pseudo-communication between nerve cells, cumulatively, altering the activities of the brain¹⁰.

The endogenous cannabinoid system (ECS) found within the brain is the major signalling pathway for THC activity¹¹. In this signalling system, THC acts via binding and modulation of the cannabinoid-1 and 2 (CB1 & 2) receptors of the prefrontal, cerebellar, basal ganglia, temporal, and hippocampal regions of the brain¹². These parts are responsible for the coordination of cognitive functions such as psychomotor performance, responsiveness, memory, learning. While a decrease in the activities of these regions is observed upon acute use¹³, chronic users are susceptible to developing neurocognitive deficits and poor behavioural engagements¹⁴.

Studies have not only demonstrated the immediate effect of cannabis but also the long-term effect on

Cite this article: Christina P, Halimat Y L, Nosipho W S, Usman A S, Saheed S. Mechanistic Insights on the Neuro-Modulatory Potential of *Cannabis sativa*: A Network Pharmacology- and Molecular Dynamics Simulation-Based Approach. Pharmacogn J. 2025;17(4): 407-419.

brain networks, morphology, and function¹⁵, the medical relevance of monitored cannabis use against neurodegenerative diseases as well as its detrimental adverse effects against the brain stemming from chronic use and abuse^{16,17}. Presently, there is scarcity of information on the neuro-modulatory effects of cannabis through its association with neurotransmitters of the central nervous system (CNS), using computational methods. Network pharmacology, a technique used to elicit the intercalation of multiple genes and compounds¹⁸ was employed to understand the intricacies of cannabis with respect to neurotransmitters' uptake, release, inhibition, and their neurological effects. Additionally, insights into the binding affinity of metabolites to targets were studied using molecular docking and dynamics simulation approaches¹⁹. Thus, these computational approaches were employed to explore the neuro-modulatory role of cannabis through its association with neurotransmitters of the CNS and uncover the mechanism by which *C. sativa* metabolites may temporarily alleviate depression, induce euphoria and from its chronic use, trigger neurological defects.

METHODOLOGY

Data mining and drug-likeness filtering of *C. sativa* metabolites

A total of 156 *C. sativa* metabolites were obtained from PubMed database (<https://pubmed.ncbi.nlm.nih.gov/>) (Supplementary Table 1). Pharmacokinetic screening of cannabis metabolites was done with the SWISSADME server (<http://www.swissadme.ch/>)²⁰ [Accessed 13th September 2023] and validated using the Moinspiration server (<https://www.molinspiration.com/cgi-bin/properties>) [Accessed 17th September 2023].

Acquisition and preparation of cannabis metabolites and neurotransmitter genes

Genes associated with each *C. sativa* metabolites were obtained by integrating their Simplified Molecular Input Line Entry System (SMILES) within the Swiss Target Prediction (STP) (<http://www.swisstargetprediction.ch/>) and Similarity Ensemble Approach (SEA) databases (<http://sea.bkslab.org/>). The Online Mendelian Inheritance in Man (<https://www.omim.org/>) [Accessed 20th September 2023] and GeneCards (<https://www.genecards.org/>) [Accessed 20th September 2023] databases were employed in the acquisition of neurotransmitter genes of the central nervous system (CNS). The Venny 2.1 (<https://bioinfo.gp.cnb.csic.es/tools/venny/>) [Accessed 30th September 2023] was used to identify common targets between cannabis metabolites and neurotransmitters²¹.

Construction of the protein-protein interaction and pathway-compound-target network

The protein-protein interactions (PPI) of the common targets were constructed with the Search Tool for the Retrieval of Interacting Genes (STRING) (<https://string-db.org/>) using protein queries for *Homo sapiens* and visualized using Cytoscape v3.8.2²². The network and integral genes analysis were done using the degree algorithm (Equation 1)

$$Deg(v) = \frac{1}{N} \dots \dots \dots (1)$$

$N(v)$ = a node neighbour, v = each node's neighbours [30].

Assessing the Kyoto Encyclopaedia of Genes and Genomes (KEGG) Pathways and Gene Ontology (GO) of common targets

The Database for Annotation, Visualization and Integrated Discovery (DAVID) tool (<https://david.ncicrf.gov/tools.jsp>) was utilized for GO analysis. For the KEGG pathway analysis, a P-value benchmark <0.05 and false discovery rate (FDR) method was employed, with the pathway producing the least FDR taken further in the study. The GO and KEGG results were visualised using an enriched bar chart and bubble plot, respectively, extrapolated from the SRC bioinformatics database (<https://www.bioinformatics.com.cn/>).

Molecular docking and molecular dynamics (MD) simulation of *C. sativa* metabolites and the enriched genes

Molecular docking studies were conducted in accordance with the study of Balogun et al²³. Briefly, 3D structures of the hub targets *CNR1* [PDB:5U09] and *GRM2* [PDB:4XAS] obtained from the most significant pathway were acquired from Protein Data Bank (<https://www.rcsb.org/>) [Accessed 15th October 2023]. Following their acquisition, USCF Chimera v1.16 was used to optimize the genes. Cannabis metabolites interacting with *CNR1* and *GRM2*, and the reference standard anti-depressant drug; anandamide²⁴ were downloaded as 3D conformers (SDF format) from PubChem database (<https://pubchem.ncbi.nlm.nih.gov/>) [Accessed 15th October 2023].

The Open Babel program plug-in on Python v0.9.5 (PyRx)²⁵, was employed to optimize metabolites. Amino acids situated at the active site of target genes *CNR1* and *GRM2* were selected to ensure binding at the active site. Coordinates were consistent and validated using Discovery Studio v21.1.0²⁶. Ligands were docked using PyRx and the top five complexes with lower docking scores and interactions were

Table 1. Docking scores (kcal/mol) and thermodynamic energy components (kcal/mol) of the top five interacting cannabis metabolites with *CNR1* and *GRM2*

Metabolites	D/S	ΔE_{vdW}	ΔE_{elec}	ΔG_{gas}	ΔG_{solv}	ΔG_{bind}
CNR1						
Campesterol	-10.9	-64.79 ± 2.86	-5.55 ± 2.27	-70.68 ± 3.29	4.72 ± 2.04	-65.95 ± 3.44
Cholesterol	-10.8	-65.99 ± 3.57	-15.39 ± 4.48	-81.75 ± 4.73	7.88 ± 2.53	-73.88 ± 4.72
Dehydrocannabifuran	-9.5	-52.56 ± 2.33	-3.47 ± 1.20	-56.03 ± 2.46	6.76 ± 1.09	-49.26 ± 2.47
Delta-8-tetrahydrocannabinolic acid	-9.6	-52.69 ± 3.12	-11.69 ± 5.28	-64.38 ± 5.42	13.91 ± 2.84	-50.47 ± 3.85
Tetrahydrocannabiphorol	-9.8	-56.33 ± 2.97	-3.63 ± 2.59	-59.97 ± 3.41	7.47 ± 1.70	-52.49 ± 3.78
Anandamide	-7.6	-59.14 ± 3.47	-32.58 ± 6.20	-91.72 ± 6.61	26.64 ± 4.02	-65.08 ± 4.51
GRM2						
4-Hydroxy-benzoic-acid	-7.0	-17.76 ± 3.02	-23.63 ± 8.78	-41.39 ± 4.96	19.89 ± 5.00	-21.5 ± 3.78
Benzyl acetate	-7.1	-24.49 ± 2.31	-8.81 ± 3.24	-33.30 ± 4.19	14.45 ± 1.92	-18.85 ± 3.87
Isolinolenic acid	-7.2	-37.65 ± 7.32	-23.78 ± 11.51	-61.43 ± 10.31	28.75 ± 8.90	-32.68 ± 7.96
Nerolidol	-7.6	-42.76 ± 2.44	-17.48 ± 3.05	-60.24 ± 3.43	16.68 ± 1.77	-43.57 ± 3.66
Pulegone	-7.3	-24.66 ± 2.61	-3.98 ± 4.55	-28.64 ± 5.37	8.94 ± 3.59	-19.7 ± 2.98
Anandamide	-6.5	-60.80 ± 3.37	-28.79 ± 7.95	-89.6 ± 7.25	30.82 ± 5.93	-58.78 ± 4.2

selected. The docking protocol was validated by assessing the binding conformations and root mean square deviation (RMSD) of the top five complexes and reference standard from the binding pockets of native inhibitors after optimal superimposition (Supplementary Figure 1)²⁷.

The AMBER 18 package (graphical processing unit version) with features including Force Field with FF18SB variant, General Amber Force Field (GAFF), and Restrained Electrostatic Potential (RESP) of the Centre for High Performance Computing (CHPC), Cape Town, South Africa was utilized for the MD simulation^{28,29}. Molecular mechanics with generalized born surface area (MMGBSA) was used to calculate the energy framework after the 200 ns simulation trajectory. The post-dynamic analysis including the RMSD, root mean square fluctuation (RMSF), solvent accessible surface area (SASA) and the radius of gyration (RoG) was conducted using the CPPTRAJ module and patterns plotted using the ORIGIN software v6.0³⁰.

Quantum chemical calculations for the top cannabis metabolites

The molecular property prediction of the top metabolite for each target and anandamide was determined using DFT/B3LYP/631G/+ (d,p) basis set.³¹ The Gaussian 16 program package resident at CHPC and Gauss View V 6.0.16 were used for the optimization and visualization respectively. Thereafter, chemical descriptors were estimated³².

RESULTS

Acquisition and preparation of *C. sativa* metabolites and neurotransmitter genes

Incorporation of each of the 156 metabolites' SMILES into the STP and SEA databases, generated 1128 and 1107 genes, respectively, from which 231 common genes were detected. Exploration of the GeneCards and OMIM databases yielded 4302 and 352 genes related to neurotransmitters, respectively, of which 314 genes were found to overlap. From this, 22 genes were identified for their linkage to *C. sativa* metabolites and neurotransmitters (Figure 1).

Construction of PPI network, GO and KEGG pathway analysis

The resultant PPI network constructed from the 22 common target genes encompassed 22 nodes and 52 edges, with an average node degree of 4.73, enrichment P-value of $< 1.0 \times 10^{-16}$ and DHCR7, TAAR1, COL18A1 and KCNK2 genes as outliers (Figure 2A). The top ten biological processes (BP), cellular component (CC), and molecular function (MF) in the GO analysis were selected for visualization due to their low P-values (Figure 2B). A further probe into the most enriched BP and CC revealed adenylate cyclase-inhibiting G-protein coupled glutamate receptor signalling pathway (1.3×10^{-10}) and plasma membrane (PM) (1.5×10^{-8}) as the most enriched, respectively. Interestingly, glutamate receptor activity (2.1×10^{-17}) was found to be the most enriched molecular function (Figure 2B). The KEGG pathway enrichment analysis generated 16 signalling pathways and based on their FDR, the neuroactive ligand receptor interaction (NALR) (1.48×10^{-15}), glutamatergic synapse (7.12×10^{-13}) and phospholipase D signalling pathway (6.76×10^{-05}) were established as the top three most enriched pathways (Figure 2C and Supplementary Table 2).

Generation of PCT network

The neuroactive ligand receptor interaction pathway comprised 13 genes with TAAR1 showing no PPIs within the network (Figure 3A). The PCT network revealed that NALR associated with 121 *C. sativa* metabolites (Figure 3B). The network comprised of 136 nodes, 223 edges with an average node degree of 3.3. Network topology analysis highlighted the cannabinoid receptor 1 (CNR1) as the most significant gene within the network, interacting with 95 metabolites (Figure 3C). A notable difference was established in the number of interactions between the top two genes of the PCT network, with the second most significant gene, glutamate metabotropic receptor 2 (GRM2) interacting with 29 metabolites (Figure 3D).

Molecular docking and MD simulation studies

Following PCT generation, the top five metabolites with the least docking scores and better binding interactions with the targets relative

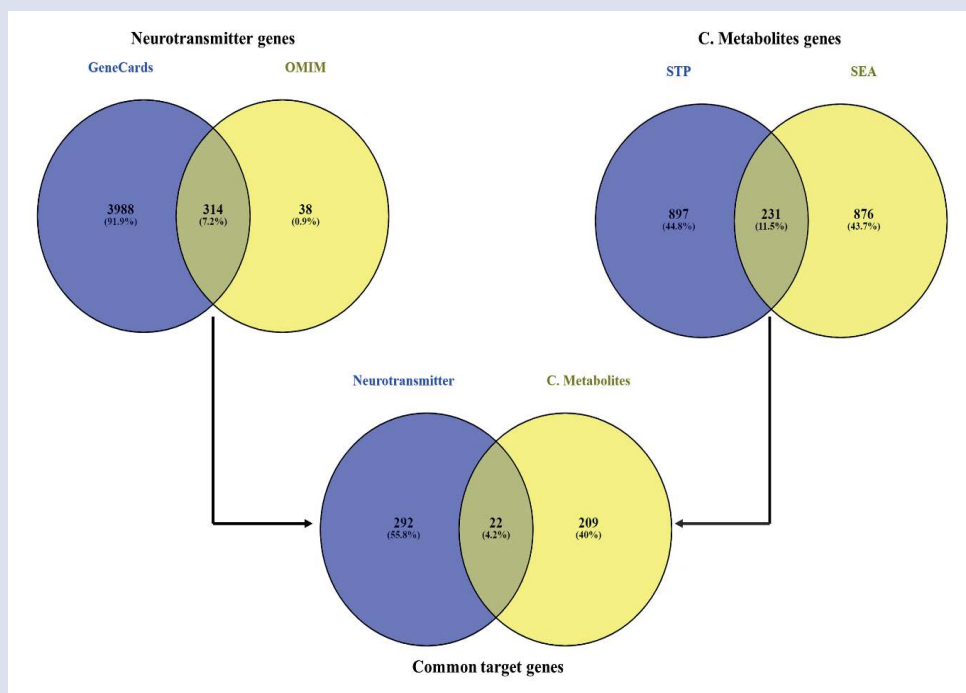


Figure 1. Common genes found between GeneCards and OMIM, SEA and STP as well as overlapping genes of *C. sativa* metabolites and neurotransmitters of the CNS.

Table 2. Average post-dynamic parameters of the top five metabolites of cannabis with CRN1 and GRM2

Complexes	RMSD (Å)	RMSF(Å)	ROG (Å)	SASA (Å)	H-bonds
CNR1					
Apo-CNR1	2.35 ± 0.41	1.69 ± 0.52	30.65 ± 0.30	20152.09 ± 304.30	209.11 ± 10.0
Campesterol	2.71 ± 0.50	1.78 ± 0.56	30.42 ± 0.28	20295.06 ± 364.54	206.07 ± 10.01
Cholesterol	2.26 ± 0.52	1.72 ± 0.59	30.38 ± 0.23	20246.53 ± 320.34	209.11 ± 9.74
Dehydrocannabifuran	2.12 ± 0.37	1.48 ± 0.47	29.97 ± 0.20	19964.38 ± 316.79	209.81 ± 9.98
Delta-8-tetrahydrocannabinolic acid	3.27 ± 0.85	1.88 ± 0.65	30.49 ± 0.28	20506.78 ± 405.16	205.53 ± 10.31
Tetrahydrocannabiphorol	2.65 ± 0.47	1.92 ± 0.64	30.60 ± 0.39	20108.05 ± 331.95	206.24 ± 9.81
Anandamide	2.52 ± 0.58	1.70 ± 0.56	30.49 ± 0.45	20008.93 ± 335.76	209.73 ± 9.88
GRM2					
Apo-GRM2	1.86 ± 0.24	1.25 ± 0.63	22.34 ± 0.13	19246.45 ± 397.1	213.84 ± 10.08
4-Hydroxy-benzoic-acid	1.98 ± 0.26	1.28 ± 0.60	22.43 ± 0.14	19578.22 ± 452.27	214.19 ± 10.37
Benzyl acetate	1.80 ± 0.23	1.26 ± 0.64	22.48 ± 0.14	19313.67 ± 421.46	213.07 ± 10.81
Isolinolenic acid	2.52 ± 0.6	1.52 ± 0.66	22.81 ± 0.33	20125.2 ± 593.62	211.63 ± 9.58
Nerolidol	1.91 ± 0.31	1.20 ± 0.82	22.21 ± 0.11	19032.26 ± 553.85	218.15 ± 10.61
Pulegone	2.05 ± 0.29	1.37 ± 0.71	22.49 ± 0.12	19708.11 ± 367.53	213.53 ± 9.89
Anandamide	2.16 ± 0.25	1.19 ± 0.59	22.58 ± 0.14	19582.62 ± 386.70	211.42 ± 9.65

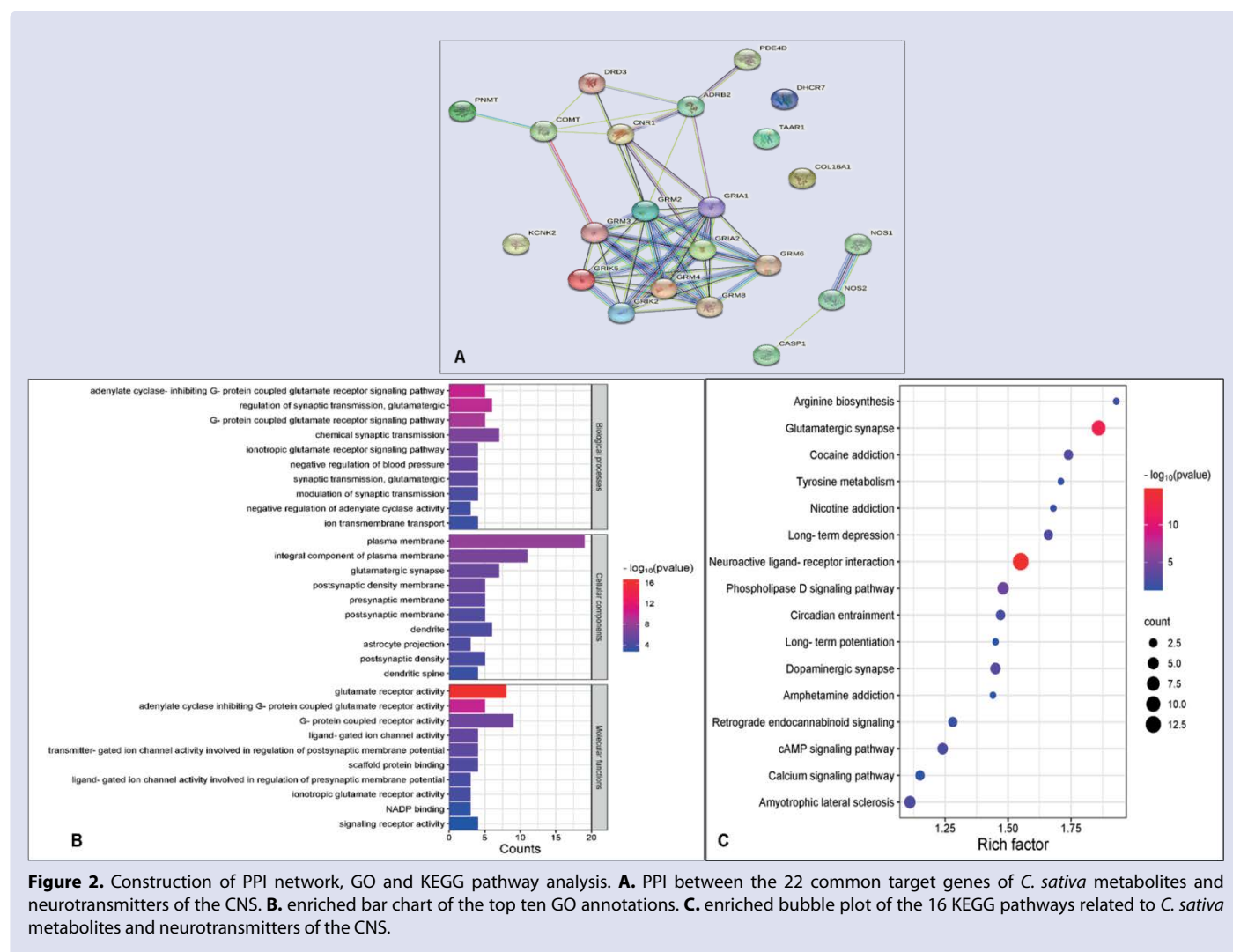


Figure 2. Construction of PPI network, GO and KEGG pathway analysis. **A.** PPI between the 22 common target genes of *C. sativa* metabolites and neurotransmitters of the CNS. **B.** enriched bar chart of the top ten GO annotations. **C.** enriched bubble plot of the 16 KEGG pathways related to *C. sativa* metabolites and neurotransmitters of the CNS.

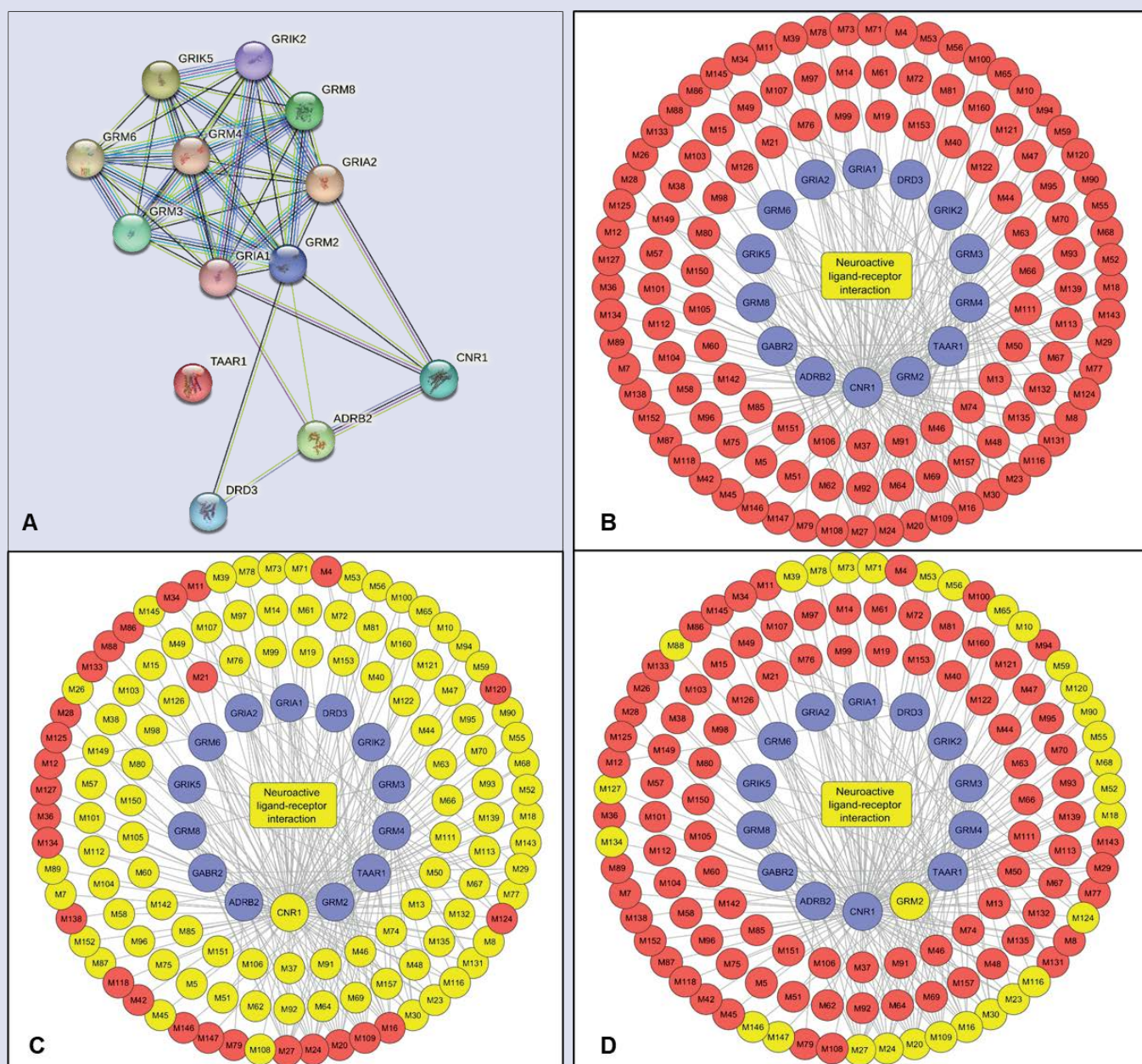


Figure 3. Network analysis of cannabis and neurotransmitter genes.

A. Gene-gene interaction of the NALR linked to *C. sativa* metabolites and neurotransmitters of the CNS **B.** Pathway-compound-target network of NALR (yellow), cannabis metabolites (red) and the common genes (blue). **C.** Pathway-compound-target network of the most significant gene [*CNR1*] of the NALR and its interacting metabolites (yellow). **D.** Pathway-compound-target network of the second most significant gene [*GRM2*] of the NALR and its interacting metabolite (yellow).

Table 3. The chemical descriptors of cannabis metabolites

Descriptors (eV)	Nerolidol	Cholesterol	Anandamide
E_LUMO	0.18	-0.16	0.1
E_HOMO	-6.09	-6.44	-6.45
Energy gap (ΔE)	6.26	6.29	6.54
Ionization energy	-0.18	0.16	-0.1
Electron affinity	6.09	6.44	6.45
Hardness	3.13	3.14	3.27
Softness	0.32	0.32	0.31
Electronegativity	2.95	3.3	3.17
Chemical potential	-2.95	-3.3	-3.17
Electrophilicity index	1.39	1.73	1.54

to the reference standard are presented in Table 1 and supplementary Tables 3 and 4. With *CNR1*, campesterol and cholesterol complexes having docking scores of -10.9 and -10.8 kcal/mol, respectively, while anandamide had -7.6 kcal/mol. With *GRM2*, nerolidol displayed the highest negative docking score of -7.6 kcal/mol followed by pulegone (-7.5 kcal/mol) while anandamide had -6.5 kcal/mol (Table 1).

The thermodynamic analysis of the complexes formed by the top five ranked metabolites of cannabis with *CNR1* and *GRM2* are presented in Table 1. The *CNR1*-cannabis metabolites complexes revealed cholesterol (-73.88 kcal/mol) and campesterol (-65.95 kcal/mol) with lower binding free energies (ΔG_{bind}) than anandamide (-65.08 kcal/mol) while the remaining three metabolites exhibited higher ΔG_{bind} than anandamide (Table 1). Relative to anandamide (58.78 kcal/mol), all *GRM2* complexes showed lower negative ΔG_{bind} . However, the *GRM2*-nerolidol complex (-43.57 kcal/mol) had the highest negative ΔG_{bind} among the investigated metabolites (Table 1).

Following equilibration of the systems during the first 5 ns, *CNR1* bound systems experienced vibrations from 1.5 Å to 5.5 Å, except campesterol. However, the systems converged at 200ns (Figure 4A). Greater vibrations of amino acid residues with prominent peaks from 25-325 residues, oscillating between 0.7 Å and 4.8 Å were observed in the RMSF plot (Figure 4B). Despite these fluctuations, the average

RMSF values of all the systems at the end of the simulation were < 2 Å. Except dehydrocannabifuran (1.48 Å), the top five cannabis metabolites had greater average RMSF values than the apo-gene (1.69 Å) and anandamide (1.70 Å) (Table 2).

The RoG plot for the *CNR1* bound system showed relatively compact complex (Figure 4C). Trajectories of the systems displayed lower RoG values than the apo-*CNR1* (30.65 Å), whereas campesterol, cholesterol, and dehydrocannabifuran complexes exhibited lower RoG values than *CNR1*-anandamide complex (Table 2). The SASA plot of *CNR1* complexes showed minimal fluctuations between 18750 Å and 22000 Å (Figure 4D) with apo-*CNR1* (20152.09 Å) presenting SASA value that was comparatively higher than anandamide and lower in cannabis metabolites-*CNR1* complexes except in dehydrocannabifuran and tetrahydrocannabinol complexes (Table 2). The intramolecular hydrogen bonds of cannabis metabolites were stable with *CNR1* (Figure 4E). The apo-*CNR1* (209.11), *CNR1*-dehydrocannabifuran (209.81) and *CNR1*-anandamide (209.73) bound systems exhibited higher hydrogen bond formation than the other complexes after the 200 ns simulation (Table 2).

Regarding *GRM2* bound systems, except for isolinolonic acid which fluctuated after the 70 ns simulation and reconverged after 140 ns, all the bound systems were relatively stable between 1.0 Å and 2.6

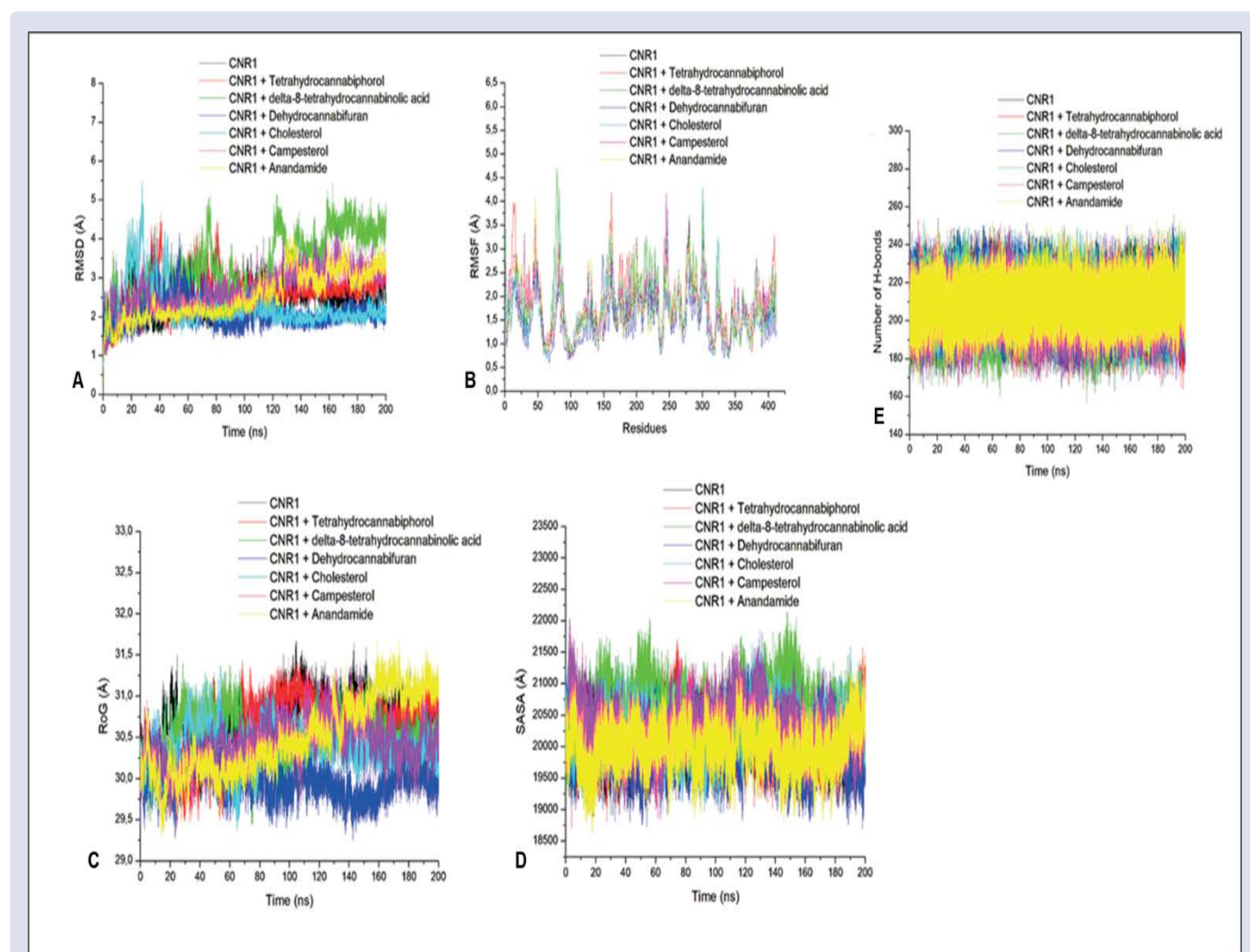


Figure 4. Comparative post-dynamic trajectories plots of the top five *C. sativa* metabolites with *CNR1*.

A. Root mean square deviation (RMSD). **B.** Root mean square fluctuation (RMSF). **C.** Radius of gyration (RoG). **D.** Solvent accessible surface area (SASA). **E.** Number of hydrogen bond.

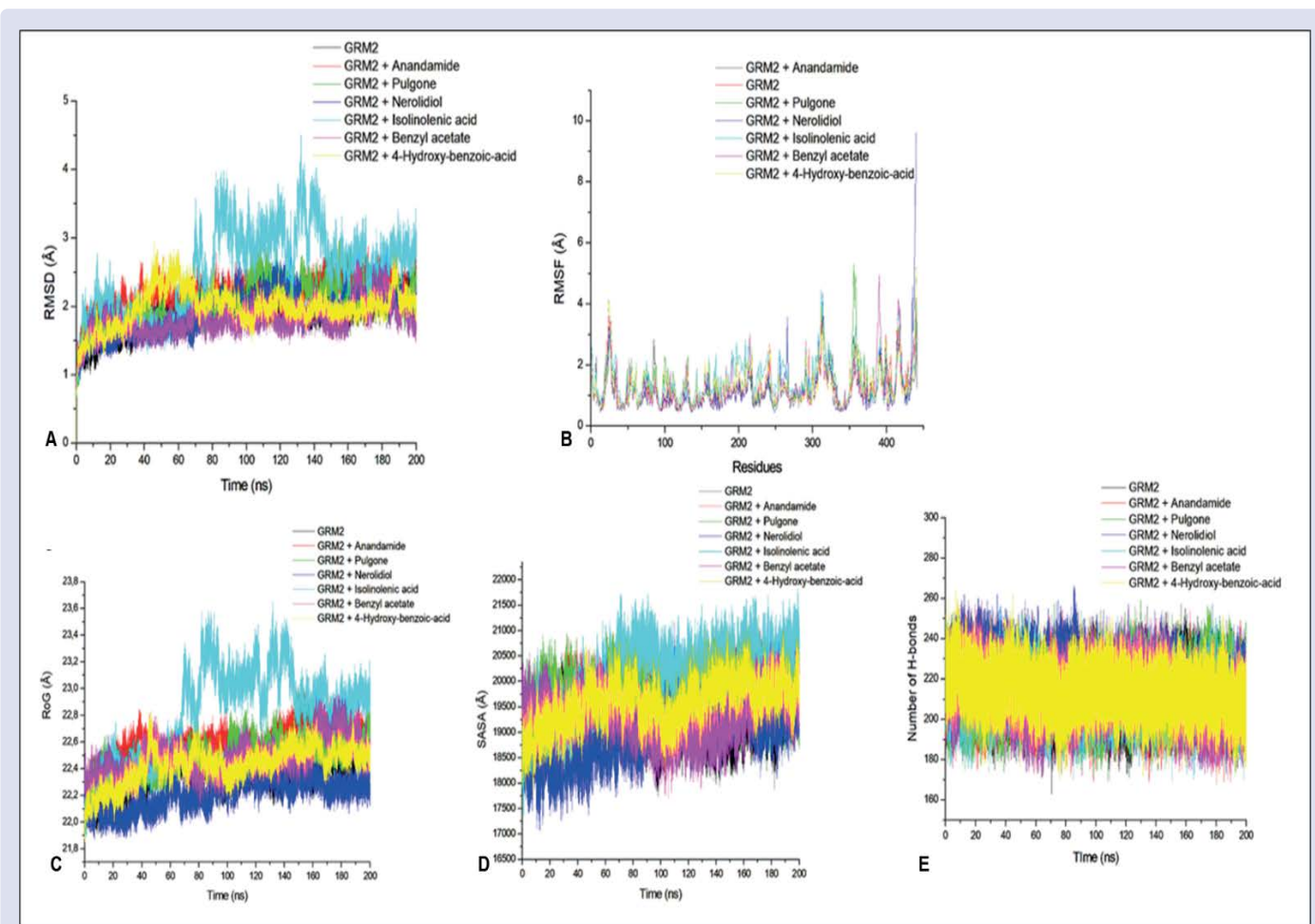


Figure 5. Comparative post-dynamic trajectories plots of the top five *C. sativa* metabolites with GRM2.

A. Root mean square deviation (RMSD). **B.** Root mean square fluctuation (RMSF). **C.** Radius of gyration (RoG). **D.** Solvent accessible surface area (SASA). **E.** Number of hydrogen bond.

Å (Figure 5A). Relative to the apo-gene (1.86 Å), GRM2-benzyl acetate complex (1.80 Å) had a lower average RMSD value unlike the remaining top four metabolites and anandamide complexes that expressed comparably higher RMSD values from 1.92 Å to 2.52 Å. (Table 2). The GRM2 complexes were relatively stable, with peak vibrations which only heightened after residue 300 (Figure 5B). Except for nerolidiol and anandamide, the average RMSF of GRM2 complexes revealed apo-GRM2 (1.25 Å) with a lower RMSF value than other top cannabis metabolites (Table 2).

In the RoG plot, apart from GRM2-isolinolenic acid complex, all the bound systems formed compact complexes with minor fluctuations observed between 21.9 Å to 22.8 Å. However, GRM2-nerolidiol complex, which initially fluctuated at 70 ns eventually stabilize at 150 ns of the simulation (Figure 5C). A comparison between the systems revealed that only GRM2-nerolidiol (22.21 Å) had lower average RoG value than apo-GRM2 (22.34 Å). Relative to GRM2-anandamide (22.58 Å) only GRM2-isolinolenic acid (22.81 Å) had a higher RoG value (Table 2). A stable SASA complex was observed all through the simulation period with isolinolenic acid diverging higher between the 60 ns to 200 ns of the simulation period (Figure 5D) with apo-GRM2 (19246.45 Å²) and GRM2-nerolidiol (19032.26 Å²) having lower average SASA values (Table 2). Similarly, a stable hydrogen bond plot was observed (Figure 5E). Apo-GRM2 (213.84) formed more hydrogen bonds than GRM2-anandamide (211.42) and cannabis metabolites except 4-hydroxybenzoic acid (214.19) and nerolidiol complexes (218.15) (Table 2).

The 2D snapshots of the top five cannabis metabolites with CNR1 over 200 ns are shown in Figure 6 and Supplementary Figure 2 while that of the top five cannabis metabolites with GRM2 are shown in Figure 7 and Supplementary Figure 3. Interactions formed between CNR1 complexes include hydrogen bonds, van der Waal, alkyl, pi-alkyl, carbon hydrogen bonds, pi-pi-stacked, pi-pi-T-shaped, pi-sulfur, pi-sigma, amide-pi stacked and unfavourable donor-donor bonds. CNR1-cholesterol formed one hydrogen bond (Ser390), which remains stable, throughout the simulation. However, as the simulation progresses, the number of hydrophobic interactions increases with residues such as Leu12, Met450, Ala446, Ile20, Phe71, Met4, Phe9, Leu453, Cys452, Val97 (Figure 6A). The CNR1-anandamide complex had a higher number of interacting residues at 200 ns, as well as better hydrogen bond formation (Ser100, ser104, Gly67 and Asp64) (Figure 6B).

While some bonds were retained in GRM2-nerolidiol complexes, an increase in intramolecular bonds were observed. At 200 ns, three hydrogen bonds (Arg39, Ala12 and Ser97), five hydrophobic interactions (Lys331, Tyr170, Arg35, Tyr98 and Arg225) were among the 20 intramolecular bonds formed (Figure 7A). GRM2-anandamide showed a steady number of intramolecular interactions from 50 ns (28 interactions) and hydrogen bonds throughout the simulation. Hydrogen bonds at 200 ns were Asp73, Asp100 and Arg197 (Figure 7B).

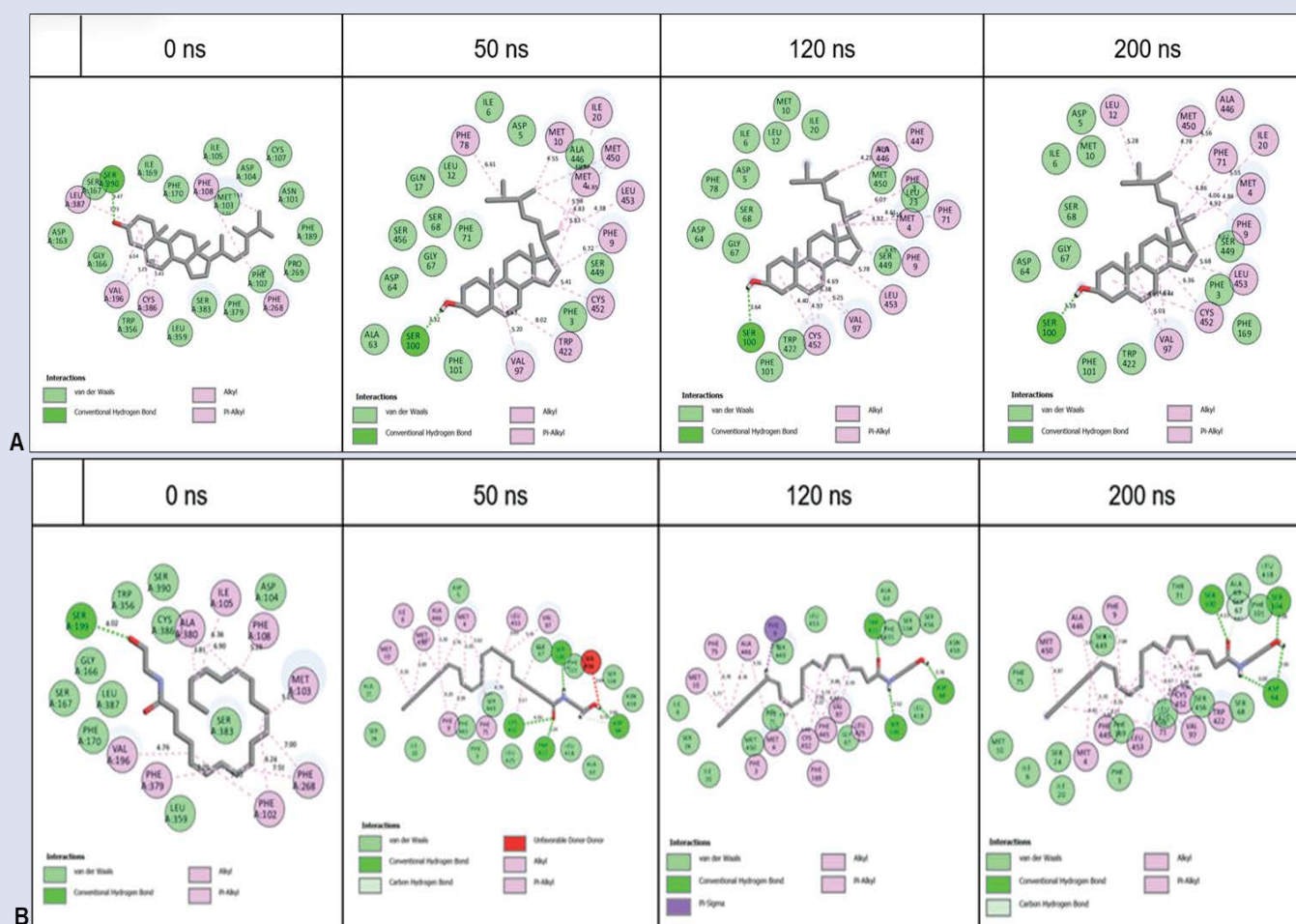


Figure 6. 2D interaction plots of top interacting metabolites and standard with *CNR1* over a 200 ns simulation period.

A. Cholesterol. **B.** Anandamide

Molecular orbital properties of the top-ranked metabolites of cannabis

The lowest unoccupied molecular orbital (LUMO) values for cholesterol and nerolidol were -0.16 eV and 0.18 eV respectively while their highest occupied molecular orbital (HOMO) values were -6.44 eV and -6.09 eV (Figure 8 and Table 3). Relative to anandamide, the metabolites had higher/lower LUMO/HOMO values. Furthermore, the anandamide presented higher energy gap (6.54 eV) than cholesterol (6.29 eV) and nerolidol (6.26 eV) and different ionization energy (-0.1 eV), hardness (3.27 eV), and lower electron affinity (6.45 eV) relative to cholesterol and nerolidol (Figure 8 and Table 3).

DISCUSSION/CONCLUSION

While cannabis has been reported as an antidepressant and implicated in neurological diseases, this study employed NP and MD simulation to understand the mechanism through which these happen. Neurotransmitters are known to communicate or send signals to nerve cells through the neuronal synapses³³. The observation that the genes of cannabis metabolites overlapped with the neurotransmitter genes is an indication that cannabis possess biological effects on the brain. This is also evident by the substantial PPI of the neurotransmitter and cannabis metabolites genes depicting a significant degree of association between both. Neurotransmitter transporters are usually available on the plasma membrane (PM) of neuronal endings either for reuptake,

or binding purposes³⁴. The finding that the PM was the most enriched cellular component in the GO emphasizes the importance of transmission of signals or NTs from one end of the neuron to another for various biological effects exhibited by cannabis.

The ECS is a member of the G-protein coupled receptor¹¹. Studies have implicated the G-protein coupled receptors as one of the ligands for glutamate in certain psychological diseases³⁵. The coupling of G- proteins to CB1 receptor leads to a reduced production of cyclic adenylylate and subsequent inhibition of Ca²⁺ channels resulting in antagonistic and hyperpolarization effects on the brain³⁶. Notably, the G-protein and adenylylate cyclase also stimulates the release of cAMP, thereby exerting modulatory effects on the cAMP signalling pathway; the dysregulation of which has been linked to major depressive disorder³⁷. In correlation, the cAMP signalling pathway was identified in the KEGG analysis; thus, its enrichment further substantiates the potential antidepressant effect of cannabis.

Amongst the KEGG pathways identified, the NALR was the most prominent based on its association with *C. sativa* metabolites. The NALR interaction reportedly exerts modulatory effects on critical psychological pathways including long term depression, through the stimulation of glutamate, noradrenaline, dopamine, and serotonin neurotransmitters³⁸. Interestingly, the glutaminergic synapse (GS) was the second most significant pathway. The GS synapses are basic synapses which allow glutamate, an excitatory neurotransmitter to

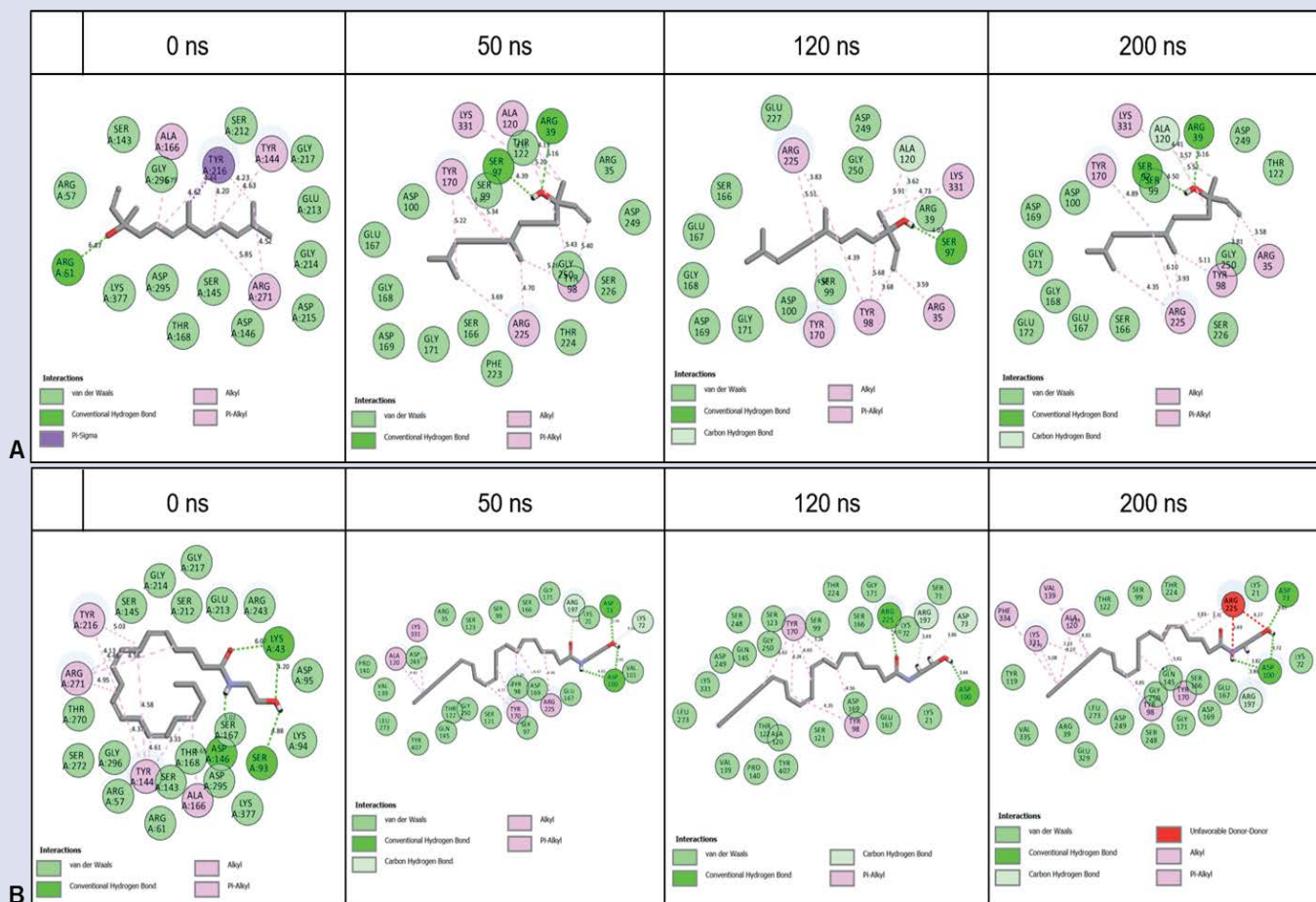


Figure 7. 2D interaction plots of top interacting metabolites and standard with *GRM2* over a 200 ns simulation period.
A. Nerolidol. **B.** Anandamide

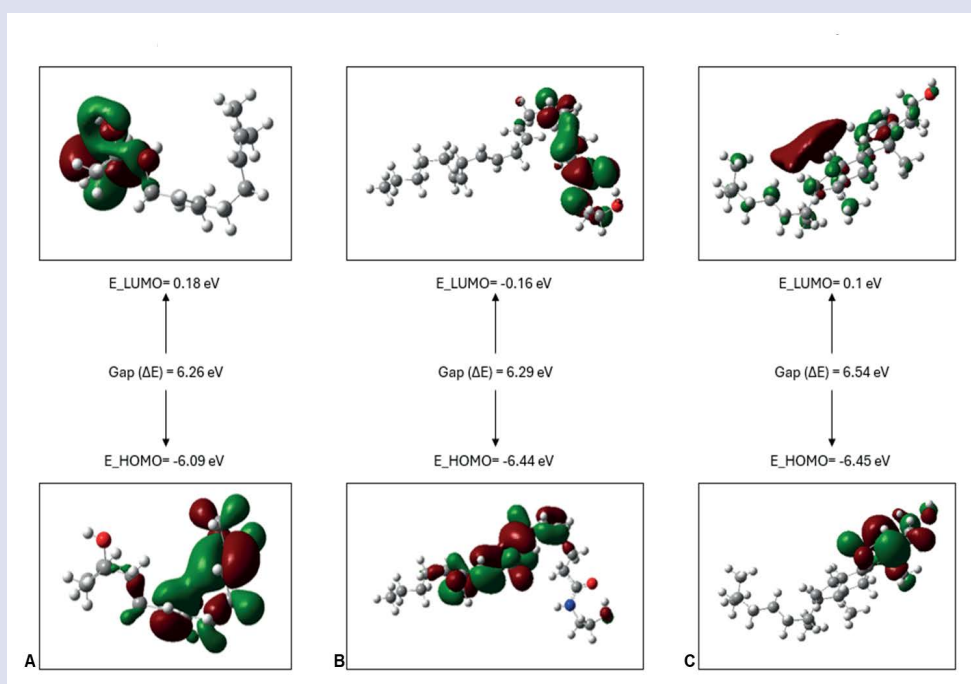


Figure 8. Transition energies of the molecular orbitals of top interacting metabolites and standard with *CNR1 GRM2*
A. Nerolidiol. **B.** Cholesterol. **C.** Anandamide

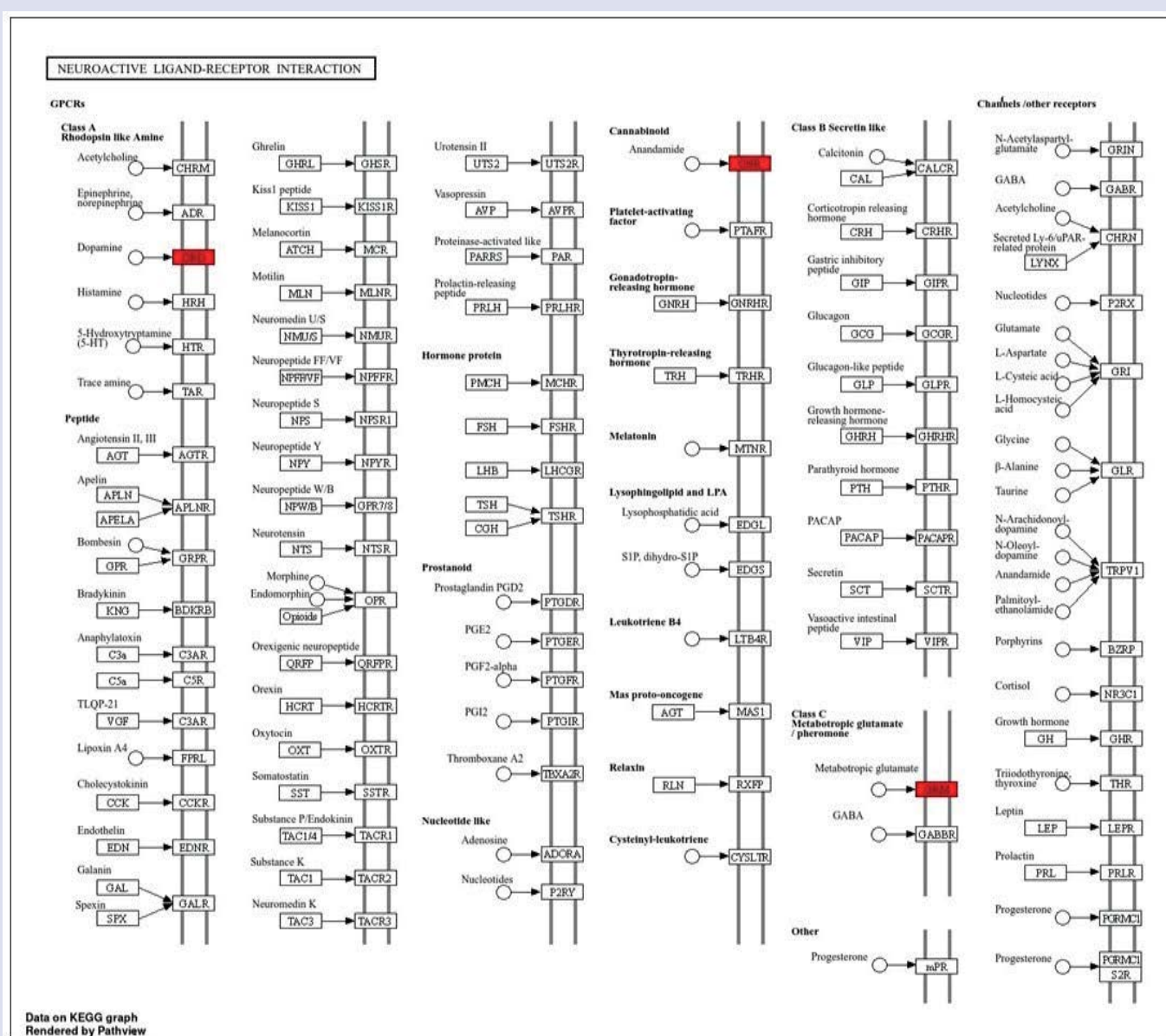


Figure 9. Enriched genes (Red) of NALR signaling pathway identified in depression and neurological disorder in this study.

Pivotal neurotransmitters (red), upon which the NALR may act through, to temporarily alleviate depression, induce euphoria and potentiate long-term neurological deficits when stimulated by *C. sativa* metabolites

be translocated from one neuron to the other³⁹. Glutamate and its mechanisms highly influence neurological functions involved in depressive phases⁴⁰. Reportedly, individuals experiencing depression are more susceptible to lower glutamate levels while excessive release contribute to neurocognitive diseases^{41,42}.

Due to its psychoactive component THC, the inhalation of cannabis causes temporary euphoria, relaxation, enhanced sensory perceptions, and increased laughter and appetite⁴³, all of which are induced by the release of neurotransmitters; dopamine, oxytocin, serotonin, and endorphins⁴⁴. Reduced dopamine level in the prefrontal cortex resulting from increased dopamine degradation is stimulated by the catechol-O-Methyltransferase gene which regulates the dopamine metabolizing enzyme and thus results in risk of psychosis⁴⁵. Noticeably, the GO and KEGG analysis pinpoint the modulatory effects of cannabis on glutamate and dopamine neurotransmitters through its association with the NALR (Figure 9).

Amongst the 14 genes involved in the NALR, *CNR1* and *GRM2* interacted with most of *C. sativa* metabolites. Cannabinoid type-1 receptor (CB1 receptor) of the ECS encoded by the *CNR1* gene is the most abundant G-protein coupled receptor located in the pre-synapse of nerve cells of the brain⁴⁶. The CB1 receptors serve as regulators capable of inhibiting the release and actions of dopamine and glutamate into synapses causing CNS dysfunction and neurological disorders⁴⁷. The observation that the *CNR1* was the most interacting gene in this study suggests that cannabis is implicated in the modulation of the CB1 receptor and the overall functioning of the brain. Furthermore, glutamate which was the most enriched molecular function in this study further suggests a network between glutamate, *CNR1* gene expression of CB1 receptor and release of glutamate relative to alleviation of depression and neuropsychological disorders.

The observation that the glutamate metabotropic receptor 2 (*GRM2*) is the second most enriched gene interacting with cannabis metabolites is

evidence of the involvement of cannabis in epigenetic modification⁴⁸. It also further coincides with the GO and KEGG analysis, linking the modulatory effects of cannabis to glutamate secretion stimulated by the neuroactive ligand receptor.

Molecular docking study was employed to assess the binding affinity of interacting *C. sativa* metabolites to the binding pocket of target receptors, with lower docking scores indicative of better binding fitness⁴⁹. The higher negative docking scores displayed by the top five *C. sativa* metabolites bound to both *CNR1* and *GRM2* potentiates better binding fitness relative to anandamide inferring a longer antidepressive effect of cannabis on its users. The low negative docking score of THC may indicate that the length of euphoric state experienced is directly proportional relationship to THC binding affinity at the *CNR1* active site. According to Campos et al⁵⁰, the use of CBD lessens depressive-like episodes, thus the lesser binding affinity of CBD to *CNR1* and *GRM2* could provide reasoning ability for the shortened relief of depression experienced by cannabis users.

Energy component calculations approximate the energy variance between bound and unbound states, with lower values indicating greater ligand-receptor affinity⁵¹. The lower docking and ΔG_{bind} of cholesterol with *CNR1* suggests its superiority against other *C. sativa* metabolites, possibly due to the presence of cholesterol within membrane rafts of the brain where receptors are situated. In correlation with the docking studies, the high negative ΔG_{bind} of nerolidol is indicative of its greater affinity for *GRM2* in comparison to other *GRM2* interacting *C. sativa* metabolites. The ΔG_{bind} of cholesterol and nerolidol emphasizes their roles as modulators of *CNR1* and *GRM2*, respectively.

The RMSD is a post-dynamic parameter that predicts the stability of a bound system by measuring the average distance between the protein backbone from its initial position to its final structural conformation, with lower values depicting greater stability⁵². Except *CNR1*-delta-8-tetrahydrocannabinolic acid complex, all systems bound to *CNR1* and *GRM2* obtained an average RMSD of <3 Å which is within the acceptable deviation limit³¹, alluding to their superior binding affinity for their respective target receptors. This might suggest that the psychoactive/antidepressant effect of cannabis wears off after some time. Nevertheless, the residual biological effect must not be undermined.

The RMSF measures ligand flexibility by enumeration residue vibrations from the initial point of complexation; RMSF values of <3.0 Å reportedly ideal for ligand flexibility³². Thus, all *C. sativa* metabolites bound to *CNR1* and *GRM2* had good flexibility, resulting in an increased binding specificity and affinity for their respective targets with *CNR1*-dehydrocannabifuran and *GRM2*-nerolidol exhibiting enhanced thermodynamic stability and flexibility resulting in a potential to exert modulatory effects on their respective targets.

The RoG measures the structural compactness and the spread of atoms during MD simulations, with higher and lower RoG values accounting for a decrease and increase in structural compactness, respectively³¹. With respect to *CNR1* and *GRM2* bound systems, differences in RoG values are negligible, resulting in the better compactness and stability of all systems, also validated by the RMSD values observed in this study. Relative to both, their apo-genes and anandamide, campesterol, cholesterol, and nerolidol bound systems, had comparable or lower RoG value indicative of their stability and potential of protein folding during complexation, thus possible higher modulatory effect than anandamide⁵².

The SASA regarded as the protein portion available to form intramolecular bonds with neighbouring ligands. Greater SASA values are indicative of more protein-environmental interactions, inciting protein instability, whereas lower SASA values alludes to

compact protein structures²⁷. Lower SASA values exhibited by *CNR1*-dehydrocannabifuran, *CNR1*-tetrahydrocannabiphrol and *GRM2*-nerolidol complexes, relative to their apo-genes and anandamide suggests their stability has probable modulators of their target receptors.

During protein-ligand binding, the rate of hydrogen bond formation influences the thermodynamic stability of the resultant complex and subsequently its biological activity⁵⁰. With respect to *CNR1*, the steady trajectories of all bound systems suggest adequate stability while the slight declining pattern of *GRM2* indicates slight reduction in hydrogen bond formation and stability. The observed differences in hydrogen bonds number in *CNR1*-cholesterol, *CNR1*-dehydrocannabifuran and *GRM2*-nerolidol relative to apo-gene and anandamide is indicative of their superior thermodynamic stability and enhanced biological activity. 2D analysis of the complexes over 200 ns revealed the presence of interactions that contribute to complex stability and affinity⁵³. Hydrogen bond is crucial for features such as binding specificity, adsorption, metabolization and other pharmacokinetic properties. The presence of hydrogen bond, particularly in the top metabolites could assist their stability and biological effects.

Quantification of metabolites HOMO and LUMO energy levels are fundamental when discerning chemical reactivity⁵⁴. Lower energy gaps influence kinetic stability, chemical hardness, and softness as well as optical polarization and are indicative of lesser stability and an increased proclivity for protein-ligand binding⁵⁴. Relative to nerolidol and cholesterol, anandamide demonstrated higher LUMO and lower HOMO values, accounting for its higher energy gap, implying lower stability over nerolidol and cholesterol. Attributed to its lower softness and higher hardness values, the less reactivity of anandamide correlated with its lower docking score, in comparison to that of nerolidol and cholesterol. Whereas the higher reactivity of nerolidol and cholesterol, concluded from its hardness and softness values may have contributed to their higher docking scores and their steady intramolecular bond formation through the 200 ns MD simulation. In tandem with its electrophilicity index, the lower electronegative value of nerolidol lessens its propensity to attract electrons³¹ thereby contributing to its lower binding free energy.

Although the correlation between the use of cannabis and cholesterol levels is yet to be fully elucidated, human and animal studies have linked cannabis intake to higher cholesterol levels⁵⁵ thereby validating its high binding affinity for *CNR1* in this study. Furthermore, this study supports the study that revealed that hypercholesterolemia is associated with Alzheimer disease⁵⁶.

The findings that cannabis metabolites significantly interacted with prominent neurotransmitter receptors that stimulates the release of glutamate and dopamine through its association with the NALR and glutaminergic synapses substantiates its potential antidepressive mechanism. The binding stability and interaction of the top five cannabis metabolites with their respective targets predicts the period of neurotransmitters modulation by cannabis during depression and in the neurological pathogenesis upon prolonged usage. While data from this study support the mechanism of neuro-modulatory effect of cannabis, the lack of preclinical and/or clinical experimentation to authenticate this via the identified hub genes of NALR forms a limitation in this study, hence, future studies to establish this is recommended.

ACKNOWLEDGMENTS

The authors wish to acknowledge the support of Directorate of Research and Postgraduate Support, Durban University of Technology, the South African Medical Research Council (SAMRC) under a Self-Initiated Research Grant, the Technology Innovative Agency and the National Research Foundation's (NRF) Competitive Programme for Rated Researchers Support (SRUG2204193723), and the International

Centre for Genetic Engineering and Biotechnology (ZAF/HDI/CRP/024) awarded to S. Sabiu. The Centre for High Performance Computing, Cape Town, South Africa is also acknowledged for the provision of computing software and modules (HEAL1361 cluster) used in this study.

REFERENCES

- Gawande VS, Deshmukh SP. Review of psychopharmacology. *GSC Biol Pharm Sci* 2023;25(2):365-371. <https://doi.org/10.30574/gscbps.2023.25.2.0456>.
- Robinson E. Psychopharmacology: From serendipitous discoveries to rationale design, but what next? *Brain Neurosci. Adv* 2018;2:2398212818812629. <https://doi.org/10.1177/2398212818812629>.
- Moncrieff J. Antidepressants: Misnamed and misrepresented. *World Psychiatry* 2015;14(3):302-303. <https://doi.org/10.1002/wps.20243>
- Alrashedy NA, Molina J. The ethnobotany of psychoactive plant use: A phylogenetic perspective. *PeerJ* 2016;4:e2546. <https://doi.org/10.7717/peerj.2546>.
- Wolinsky D, Barrett FS, Vandrey R. The psychedelic effects of cannabis: A review of the literature. *J Psychopharmacol* 2024;38(1):49-55. <https://doi.org/10.1177/02698811231209194>
- World Health Organization [<https://www.afro.who.int/health-topics/substance-abuse>]. Substance Abuse; 2023. [Cited 2024 Mar 25].
- Garcia A. State Medical Marijuana Laws. [NCSL Website]. 2021. Available at: www.ncsl.org/research/health/state-medical-marijuana-laws.aspx.
- Chayasisobhon S. Mechanisms of action and pharmacokinetics of cannabis. *Perm J* 2020;25:1-3. <https://doi.org/10.7812/TPP/19.200>.
- Khalsa JH, Bunt G, Blum K, Maggirwar SB, Galanter M, Potenza MN. Cannabinoids as Medicinals. *Curr Addict Rep* 2022;9(4):630-646. <https://doi.org/10.1007/s40429-022-00438-3>.
- National Institute on Drug Abuse [<https://nida.nih.gov/publications/drugs-brains-behavior-science-addiction/drugs-brain>] 2022. Drugs and the Brain. [Updated 2024 Mar 16; cited 2024 Mar 25]
- Lutz B. Neurobiology of cannabinoid receptor signaling. *Dialogues Clin Neurosci* 2020;22(3):207-222. <https://doi.org/10.31887/DCNS.2020.22.3/blutz>
- Brunt TM, Bossong MG. The neuropharmacology of cannabinoid receptor ligands in central signaling pathways. *Eur J Neurosci* 2022;55(4):909-921. <https://doi.org/10.1111/ejn.14982>
- Brumback T, Castro N, Jacobus J, Tapert S. Effects of marijuana use on brain structure and function: Neuroimaging findings from a neurodevelopmental perspective. *Int Rev Neurobiol* 2016;129:33-65. <https://doi.org/10.1016/bs.irn.2016.06.004>
- Mercuri K, Terrett G, Henry JD, Curran HV, Elliott M, Rendell PG. Episodic foresight deficits in regular, but not recreational, cannabis users. *J Psychopharmacol* 2018;32(8):876-882. <https://doi.org/10.1177/0269881118776672>
- Soleimani N, Kazemi K, Helfroush MS, Aarabi A. Altered brain structural and functional connectivity in cannabis users. *Sci Rep* 2023;13(1):5847. <https://doi.org/10.1038/s41598-023-32521-8>
- Cassano T, Villani R, Pace L, Carbone A, Bukke VN, Orkisz S, et al. From *Cannabis sativa* to cannabidiol: Promising therapeutic candidate for the treatment of neurodegenerative diseases. *Front Pharmacol* 2020;11:124. <https://doi.org/10.3389/fphar.2020.00124>
- Burggren AC, Shirazi A, Ginder N, London ED. Cannabis effects on brain structure, function, and cognition: Considerations for medical uses of cannabis and its derivatives. *Am J Drug Alcohol Abuse* 2019;45(6):563-579. <https://doi.org/10.1080/00952990.2019.1634086>
- Guo W, Huang J, Wang N, Tan HY, Cheung F, Chen F, et al. Integrating network pharmacology and pharmacological evaluation for deciphering the action mechanism of herbal formula zuojin pill in suppressing hepatocellular carcinoma. *Front Pharmacol* 2019;10:466724. <https://doi.org/10.3389/fphar.2019.01185>.
- Akoonjee A, Rampadarath A, Aruwa CE, Ajiboye TA, Ajao, AA, Sabiu S. Network pharmacology-and molecular dynamics simulation-based bioprospection of *Aspalathus linearis* for type-2 diabetes care. *Metabolites* 2022;12(11):1013. <https://doi.org/10.3390/metabo12111013>.
- Daina A, Michielin O, Zoete V. SwissADME: a free web tool to evaluate pharmacokinetics, drug-likeness and medicinal chemistry friendliness of small molecules. *Sci Rep* 2017;7(1):42717. <https://doi.org/10.1038/srep42717>.
- Oh KK, Adnan M, Cho DH. Network pharmacology of bioactives from Sorghum bicolor with targets related to diabetes mellitus. *PLoS One* 2020;15(12):e0240873. <https://doi.org/10.1371/journal.pone.0240873>
- Shannon P, Markiel A, Ozier O, Baliga NS, Wang JT, Ramage D, et al. Cytoscape: a software environment for integrated models of biomolecular interaction networks. *Genome Res* 2003;13(11):2498-2504. <https://doi.org/10.1101/gr.1239303>.
- Balogun FO, Naidoo K, Aribisala JO, Pillay C, Sabiu S. Cheminformatics Identification and validation of dipeptidyl peptidase-iv modulators from shikimate pathway-derived phenolic acids towards interventional type-2 diabetes therapy. *Metabolites* 2022;12(10):937. <https://doi.org/10.3390/metabo12100937>
- Gobbi G, Bambico FR, Mangieri R, Bortolato M, Campolongo P, Solinas M, et al. Antidepressant-like activity and modulation of brain monoaminergic transmission by blockade of anandamide hydrolysis. *Proceedings of the National Academy of Sciences of the United States of America* 2002;102(51):18620–18625. <https://doi.org/10.1073/pnas.0509591102>
- Dallakyan S, Olson AJ. Small-molecule library screening by docking with PyRx. *Methods Mol Biol* 2015;1263:243-250. https://doi.org/10.1007/978-1-4939-2269-7_19
- BIOVIA DS. Discovery Studio, version 21.1.0. San Diego: Dassault Systèmes 2021;627
- Mpofana N, Peter C, Lukman HY, Makgobele MU, Dlov NC, Gqaleni N, et al. Mechanisms of Selected Cassipourea Metabolites for Melasma Treatment: Network Pharmacology and Molecular Dynamics Study. *F1000Research* 2024;13:952. <https://doi.org/10.12688/f1000research.153996.1>
- Nair PC, Miners JO. Molecular dynamics simulations: From structure function relationships to drug discovery. In *Silico Pharmacol* 2014;2:1-4. <https://doi.org/10.1186/s40203-014-0004-8>
- Seifert E. OriginPro 9.1: scientific data analysis and graphing software-software review. *J Chem Inf Model* 2014;54(5):1552. <https://doi.org/10.1021/ci500161d>.
- Gonnet P. P-SHAKE: a quadratically convergent SHAKE in O (n2). *J Comput Phys* 207;220(2):740-750.
- Lukman HY, Aribisala JO, Akoonjee A, Sulyman AO, Wudil AM, Sabiu S. Modulation of dipeptidyl peptidase by Rooibos tea metabolites towards type 2 diabetes care: Evidence from molecular dynamics simulation and density functional theory. *Sci Afr* 2024;e02173. <https://doi.org/10.1016/j.sciaf.2024.e02173>
- Lanrewaju AA, Enitan-Folami AM, Nyaga MM, Sabiu S, Swalaha FM. Cheminformatics bioprospection of selected medicinal plants metabolites against trypsin cleaved VP4 (spike protein) of rotavirus A. *J Biomol Struct Dyn* 2023;1-20. <https://doi.org/10.1080/07391102.2023.2258405>.
- Teleanu RI, Niculescu AG, Roza E, Vladăcenco O, Grumezescu AM, Teleanu DM. Neurotransmitters-Key Factors in Neurological and Neurodegenerative Disorders of the Central Nervous System. *Int J Mol Sci* 2022;23(11):5954. <https://doi.org/10.3390/ijms23115954>.

34. Oliveira TG, Di Paolo G. Phospholipase D in brain function and Alzheimer's disease. *Biochimica et biophysica acta* 2010;1801(8):799–805. <https://doi.org/10.1016/j.bbali.2010.04.004>.
35. Ebrahimi-Ghiri M, Khakpai F, Zarrindast MR. Combined treatment of scopolamine and group III mGluR antagonist, CPPG, exerts antidepressant activity without affecting anxiety-related behaviors. *Physiol behave* 2020;224:113034. <https://doi.org/10.1016/j.physbeh.2020.113034>.
36. Pertwee RG, Howlett AC, Abood ME, Alexander SP, Di Marzo V, Elphick MR, et al. International Union of Basic and Clinical Pharmacology. LXXIX. Cannabinoid receptors and their ligands: beyond CB1 and CB2. *Pharmacol Rev* 2010;62(4):588–631. <https://doi.org/10.1124/pr.110.003004>.
37. Ho CSH, Soh MWT, Tay GWN. The diagnostic utility of miRNA and elucidation of pathological mechanisms in major depressive disorder. *Compr Psychiatry* 2023;121:152363. <https://doi.org/10.1016/j.comppsych.2022.152363>.
38. Huang C, Zheng C, Li Y, Wang Y, Lu A, Yang L. Systems pharmacology in drug discovery and therapeutic insight for herbal medicines. *Brief Bioinform* 2014;15(5):710–733. <https://doi.org/10.1093/bib/bbt035>
39. Di Maio V. The glutamatergic synapse: A complex machinery for information processing. *Cogn Neurodyn* 2021;15(5):757–781. <https://doi.org/10.1007/s11571-021-09679-w>.
40. Khodoruth MAS, Estudillo-Guerra MA, Pacheco-Barrios K, Nyundo A, Chapa-Koloffon G, Ouanes S. Glutamatergic system in depression and its role in neuromodulatory techniques optimization. *Frontiers Psychiatry* 2022;13:886918. <https://doi.org/10.3389/fpsy.2022.886918>.
41. Kryszkowski W, Boczek T. The G protein-coupled glutamate receptors as novel molecular targets in schizophrenia treatment: A narrative review. *J Clin Med* 2021;10(7): 1475. <https://doi.org/10.3390/jcm10071475>.
42. Onalapo AY, Onalapo OJ. Glutamate and depression: Reflecting a deepening knowledge of the gut and brain effects of a ubiquitous molecule. *World J Psychiatry* 2021;11(7):297. <https://doi.org/10.5498/wjp.v11.i7.297>
43. National Institute on Drug Abuse (NIDA). What are marijuana's effects? 2021. <https://nida.nih.gov/publications/research-reports/marijuana/what-are-marijuana-effects>. [Last accessed: 03/25/2024].
44. Pareek A, Satapathy SK. Productivity Sustenance with Effectiveness of Work Circles: A Study on the "Happy Hormones". In: Resource efficiency, sustainability, and globalization. Apple Academic Press 2021; pp. 41–59.
45. Grechuk K, Azizi H, Sharma V, Khan T, Jolayemi A. Cannabis, Schizophrenia Risk and Genetics: A Case Report of a Patient with Homozygous Valine Catechol-O-Methyltransferase Polymorphism. *Cureus* 2021;13(6):e15740. <https://doi.org/10.7759/cureus.15740>.
46. Zou S, Kumar U. Cannabinoid receptors and the endocannabinoid system: signaling and function in the central nervous system. *Int J Mol Sci* 2018;19(3):833. <https://doi.org/10.3390/ijms19030833>.
47. Sultan AA, Dimick MK, Zai CC, Kennedy JL, MacIntosh BJ, Goldstein BI. The association of *CNR1* genetic variants with resting-state functional connectivity in youth bipolar disorder. *Eur Neuropsychopharmacol* 2023;71:41–54. <https://doi.org/10.1016/j.euroneuro.2023.03.004>
48. Alameda L, Trotta G, Quigley H, Rodriguez V, Gadelrab R, Dwir D, et al. Can epigenetics shine a light on the biological pathways underlying major mental disorders? *Psychol med* 2022;52(9):1645–1665. <https://doi.org/10.1017/S0033291721005559>.
49. Shode FO, Uhomobhi JO, Idowu KA, Sabiu S, Govender KK. Molecular dynamics study on selected bioactive phytochemicals as potential inhibitors of HIV-1 subtype C protease. *Metabolites* 2022;12(11):1155. <https://doi.org/10.3390/metabo12111155>.
50. Sulyman AO, Aliyu OM., Ajani EO, Abdulkareem YF, Afe IA, Abdulyakeen FO, et al. Mechanisms of L-citrulline on phosphodiesterase 5 in erectile dysfunction intervention. *Sci Afr* 2025;27:e02572. <https://doi.org/10.1016/j.sciaf.2025.e02572>
51. Akoopjee A, Lukman HY, Ajao AA, Uthman TO, Sabiu S. A network pharmacology- and molecular dynamics simulation-based bioprospection of *Khaya grandifoliola* C. DC. for diabetes care. *J Biomol Struct Dyn* 2024;1–20. <https://doi.org/10.1080/07391102.2024.2446672>
52. Campos AC, Fogaça MV, Sonogo AB, Guimarães FS. Cannabidiol, neuroprotection and neuropsychiatric disorders. *Pharmacol Res* 2016;112:119–127. <https://doi.org/10.1016/j.phrs.2016.01.033>.
53. S'thebe NW, Aribisala JO, Sabiu S. Cheminformatics bioprospection of sunflower seeds' oils against quorum sensing system of *Pseudomonas aeruginosa*. *Antibiotics* 2023;12(3):504. <https://doi.org/10.3390/antibiotics12030504>
54. Akintemi EO, Govender KK, Singh T. A DFT study of the chemical reactivity properties, spectroscopy, and bioactivity scores of bioactive flavonols. *Comput Theor Chem* 2022;1210:113658. <https://doi.org/10.1016/j.comptc.2022.113658>.
55. Dabiri AE, Kassab GS. Effects of cannabis on cardiovascular system: the good, the bad, and the many unknowns. *Med Cannabis Cannabinoids* 2021;4(2):75–85. <https://doi.org/10.1159/000519775>.
56. Hayatghaybi H, Karimi I. Hypercholesterolemic effect of drug-type *Cannabis sativa* L. seed (marijuana seed) in guinea pig. *Pak J Nut* 2007; 6:56–59.

Cite this article: Christina P, Halimat Y L, Nosipho W S, Usman A S, Saheed S. Mechanistic Insights on the Neuro-Modulatory Potential of *Cannabis sativa*: A Network Pharmacology- and Molecular Dynamics Simulation-Based Approach. *Pharmacogn J.* 2025;17(4): 407–419.